




Pressure-Pipe Breaks Relationship in Water Distribution Networks: A Statistical Analysis

Iman Moslehi¹  · Mohammadreza Jalili_Ghazizadeh¹

Received: 5 October 2018 / Accepted: 27 May 2020 /
Published online: 27 June 2020
© Springer Nature B.V. 2020

Abstract

Maximum pressure is a crucial factor in pipe break events. In this paper, a field data-based methodology is proposed to statistically investigate the relationship between operating pressures and pipe break rates in water distribution networks. The objective is to develop the pipe break rate functions (BRFs) where a maximum pressure indicator (MPI) is associated with an average level of pipe break rates. The methodology uses measured pressure values at the average zone point to calculate MPIs along with recorded pipe breaks to establish BRFs for different pipe materials. The Bayes theorem is then applied to identify the maximum pressure thresholds on the BRFs by means of the unconditional and break- conditioned cumulative distribution functions of the MPIs. The methodology is applied to a large zone of the water distribution network of Tehran (Iran). The results showed that the annual average of the MPI is the best indicator to develop BRFs. The obtained pressure thresholds confirm that the break rates increase rapidly for specific maximum pressure ranges, which can be used to implement effective pressure management.

Keywords Break rate function · Bayes theorem · Maximum pressure · Pressure management · Statistical analysis

1 Introduction

Frequent pipe breaks in water distribution networks (WDNs) are one of the major challenges facing water utilities worldwide (Ghorbanian et al. 2015). This issue can cause high direct and indirect economic, environmental and social costs and remains a significant concern due to

✉ Iman Moslehi
i_moslehi@sbu.ac.ir

Mohammadreza Jalili_Ghazizadeh
m_jalili@sbu.ac.ir

¹ Department of Civil, Water and Environmental Engineering, Shahid Beheshti University, Tehran, Iran

some adverse consequences, including water and energy losses, substantial repair cost, service level interruptions, traffic delays, and water contamination in distribution networks. Besides, the majority of water utilities are operating under limited budgets and scarce capital resources. Therefore, as substantial investment is required to renew and replace pipe networks, pipe breaks should be avoided as great an extent as possible (Martínez-Codina et al. 2015).

For all these reasons, Several predictive break models have been developed to assist water utilities for future planning, prioritizing and decision-making of maintenance, rehabilitation, and replacement (M/R/R) activities (Kabir et al. 2015, 2016; Kakoudakis et al. 2017). These models can be classified into physical and statistical models (Kleiner and Rajani 2001; Nishiyama and Fillion 2013). Physical models attempt to model the physical mechanisms of pipe breaks which are often very complex to be completely understood (Rajani and Kleiner 2001).

The statistical models have been developed to identify patterns of pipe breaks and failure behaviors based on historical data of pipe breaks. These models can be applied with various levels of input data, even when few data is available (Kleiner and Rajani 2001; Nishiyama and Fillion 2013; Scheidegger et al. 2015). Besides the statistical models, a number of newer methods have been employed based on data mining techniques due to the complexity of water networks (Berardi et al. 2008; Xu et al. 2011). These methods include techniques like artificial neural networks (Jafar et al. 2010; Shirzad et al. 2014; Kutyłowska 2015), genetic programming (Babovic et al. 2002; Xu et al. 2011) and evolutionary polynomial regression (Giustolisi and Savić 2006, 2009; Berardi et al. 2008; Kakoudakis et al. 2017).

Input variables in the statistical models may be referred to as effective factors that contribute to unintentional pipe breaks and affect breakage rates. These factors can be classified into three main categories: physical, operational, and environmental factors (Kleiner and Rajani 2001; Al-Barqawi and Zayed 2006). They include pipe age, pipe material, pipe diameter, soil type, traffic loading, water pressure, water quality, and climatic conditions such as temperature, rainfall, and groundwater condition. It should be noted that pipe break data are often needed to be segregated to homogenous groups with similar properties (operational, environmental and physical) to better identify breakage patterns and to obtain statistical significance (Kleiner and Rajani 2001; Xu et al. 2011).

Water pressure is one of the main operational factors contributing to the break rates of pipes in water networks and there is a direct link between the occurrence of pipe break and operating pressures. Several researchers have emphasized that high pressure has a substantial influence on pipe break rates (Pearson et al. 2005; Thornton and Lambert 2005, 2007; Martínez-Codina et al. 2015). It has been consistently reported in the literature that the frequency of pipe breaks significantly reduced after implementation of pressure management (PM) in many WDNs throughout the world (Lambert 2002; Thornton and Lambert 2006, 2007; Girard and Stewart 2007; Palau et al. 2012). PM is usually associated with maximum pressure control using pressure-regulating valves (PRVs) in order to reduce excessive pressure at certain times of the day. In addition, the effectiveness of implementing PM schemes mainly depends on the conditions of the distribution network (Thornton and Lambert 2007; Vicente et al. 2016). Therefore, the analysis of the relationship between pressure and pipe breaks is necessary for implementing effective PM schemes and prioritizing M/R/R activities.

The majority of statistical models have been focused primarily on describing pipe break rates based on a combination of effective factors contributing to pipe breaks (Berardi et al. 2008; Wang et al. 2009; Kabir et al. 2010; Xu et al. 2011). The most frequent factors have been considered to predict pipe break rates include physical and environmental factors like pipe age, pipe material, pipe length, pipe diameter, previous pipe breaks, temperature and soil corrosivity (Kleiner and

Rajani 2001; Ghorbanian et al. 2015; Kabir et al. 2015). Little effort in previous studies has been made to investigate the relationship between pressure and occurrence of pipe breaks, since it is difficult to establish such a relationship (Lambert and Fantozzi 2010; Martínez-Codina et al. 2015). Moreover, because of the scarcity of filed data, pressure in some predictive break models is often estimated by hydraulic simulation models. The estimated values of pressure may be included a degree of uncertainty, especially in large WDNs, associated with the input parameters such as water demands and hydraulic conductivity of pipes (Ghorbanian et al. 2015). This may be lead to provide imprecise results by predictive pipe break models.

The International water Association task force conducted a number of studies to demonstrate the effects of PM on reducing pipe breaks. They pointed out that pipe break frequency similar to leakage can be related to a power component of pressure (Lambert 2001; Farley and Trow 2003). Thus, the N_2 exponent was proposed to predict changes in new pipe break occurrences (B_0 to B_1) as pressure varies (P_0 to P_1) following the exponential relationship: ($B_1/B_0 = (P_1/P_0)^{N_2}$). Following studies showed N_2 values can widely vary between 0.2 and 12 for water mains and service connections, and thus, the N_2 approach for analysis of pressure-pipe break relationships was inappropriate (Pearson et al. 2005; Thornton and Lambert 2005; Lambert et al. 2013). Thornton and Lambert (2007) demonstrated that the reduction in new pipe breaks depends on the break frequency before implementing PM. They introduced a conceptual approach to provide an explanation of the variability of results between different zones in response to pressure changes (Thornton and Lambert 2007). This concept explains that the break frequency of a specified zone has a relatively low value until some particular pressure is exceeded, and then small increases in pressure may cause break frequency increases rapidly. However, they did not explain how this particular pressure ranges may be identified. A general form of equation through the use of N_2 exponent was developed to explain the conceptual approach based on the several sets of field data (Lambert and Thornton 2012).

Martínez-Codina et al. (2015) proposed a new methodology based on a Bayesian approach for identifying maximum pressure ranges that is most likely to reduce pipe breaks. The results confirmed that the probability of pipe breaks increases for specific pressure ranges. Thus, they suggested that maximum operating pressure should have an upper limit for the reduction of the probability of breaks. However, the recorded pipe breaks for all materials were used to determine pressure ranges in their study, as the number of pipe breaks for each type of pipe material was too small for statistical inference. This may produce statistical noise in data and causing imprecise results in the estimation of the probability of pipe breaks, as different pipe materials are likely to respond differently to changes in pressure (Lambert and Thornton 2011).

The main objective of this paper is to investigate the relationship between operating pressures and pipe break frequency in WDNs. A field data-based methodology is proposed to describe pressure-pipe break relationships by determining break rate functions (BRFs). Moreover, when the BRFs are established, the Bayes' theorem is applied to identify particular pressure thresholds on the BRF curves in which the pipe break rates increase rapidly for small increases in pressure. The estimated pressure ranges can assist water utilities in the implementation of effective PM for reducing pipe breaks while providing adequate service pressure. To demonstrate the applicability of the proposed methodology, it was applied to a large portion of the WDN of Tehran, Iran. This study provides a more comprehensive understanding of pressure-pipe breaks relationship in WDNs. The developed BRFs can be applied to estimate expected pipe breaks based on the probability distribution of operating pressures. The results can also be incorporated into the development of economic models to determine financial benefits of PM.

2 Methodology

It is well established that maximum operating pressure is a prime or contributory factor to the occurrences of pipe breaks in WDNs. This operational factor may cause an increase in pipe breaks coupled with the physical and environmental factors. Therefore, it is essential to establish a relationship between operating pressure and pipe breaks. The proposed methodology uses field data of pressure and recorded pipe breaks to develop such a relationship by determining BRFs. The methodology is summarized in Fig. 1, comprising three main steps. The first step includes collection and data filtering of pressure and pipe breaks. In the second step, the BRFs for different pipe materials of water mains are determined to describe the relationship between pressure and pipe break rates. Finally, the Bayes' theorem is applied in order to determine the maximum pressure thresholds on the BRF curves that could have a substantial influence on the reduction of pipe breaks.

2.1 Data Collection and Filtering

To precisely describe the relationship between pressure and pipe breaks based on BRFs, the collecting adequate field data of operating pressure and pipe breaks is important. Operating pressure in an individual zone of a WDN is characterized by means of a pressure indicator, which is defined as the calculated statistics from the time series of pressure head over a specific time window (Martínez-Codina et al. 2015). Here, instantaneous pressure values for the calculation of the pressure heads are measured at the Average Zone Point (AZP) of the study area where the pressure variations can be considered to be representative of the zone average (ILMSS 2013; Renaud et al. 2015). Subsequently, the Maximum Pressure Indicator (MPI) is calculated as the maximum value of the time series of the pressure head over the time window.

A systematic approach is applied to identify the location of the AZP at an individual zone (WSAA 2009; ILMSS 2013; Moslehi et al. 2020). First, the geographical information system (GIS) tool is exploited to calculate the weighted average ground level (WAGL) of the zone. Then, a physical point in the center of the zone is selected as AZP for pressure measurements with the same calculated WAGL. The instantaneous pressure values are measured at the AZP with regular time step (e.g., every 10-min). Finally, the time series of the hourly average pressure heads are calculated from the measured instantaneous pressure values and the set of MPI values is calculated from the hourly average pressure time series over a specific time window.

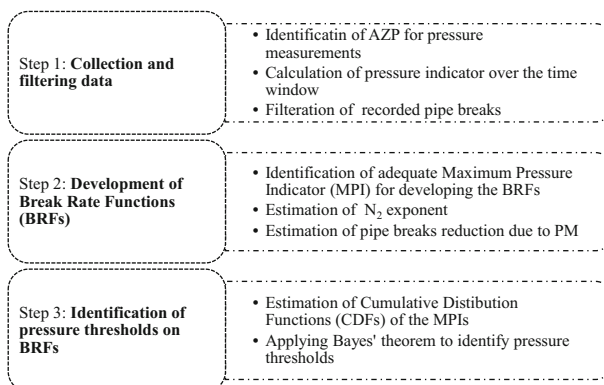


Fig. 1 The proposed methodology for developing BRFs in WDNs

Pipe breaks data is usually collected and recorded annually by the water utilities in a database. The major information about each pipe break in a database may often be included the type of repairs, causes of breaks (i.e. internal or external causes), failure modes, the location of a pipe break, the time when a pipe break is first reported and pipe characteristics such as pipe type (i.e., water main or service connection), pipe diameter and pipe material. Data filtering of recorded pipe breaks data into homogeneous groups with similar properties is necessary to use the proposed methodology, which can be based on pipe characteristics (e.g., type and material), failure modes and causes of breaks.

2.2 Development of BRFs

In the second step of the methodology, the relationship between pressure and pipe breaks is established by developing BRFs where an MPI is associated with an average level of pipe break rates (Filion et al. 2007; Ghorbanian et al. 2015). The BRF in an individual zone (as depicted in Fig. 2) can be calculated using the following equation (Lambert and Thornton 2012):

$$BRF = BF_{npd} + BF_{pd} = BF_{npd} + A \times MPI_{AZP}^{N_2} \tag{1}$$

where BF_{npd} = non-pressure dependent break rate (not influenced by pressure); BF_{pd} = pressure-dependent break rate (varies with pressure). MPI_{AZP} = the MPI value at the AZP; N_2 = the exponent of pressure-pipe break relationship. The “A” = a zone parameter influencing the curve slope in pressure-dependent part. Moreover, the following relationship can be used to assess the effect of PM on pipe break rates (Lambert and Thornton 2012):

$$R = (1 - C_b) \left(1 - \left(\frac{MPI_{AZP1}}{MPI_{AZP0}} \right)^{N_2} \right) \tag{2}$$

where R = reduction of pipe breaks due to implementing PM; C_b = the ratio of BF_{npd} part to initial break rate before PM implementation (BF_0) that varies between [0 1]; MPI_{AZP0} and MPI_{AZP1} represent the MPI values at AZP before and after PM implementation, respectively.

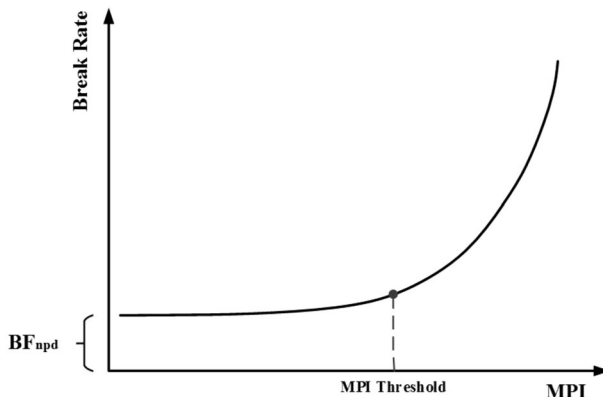


Fig. 2 The hypothetical break rate function

The BF_{npd} for an individual zone may be affected by some influential factors such as pipe age, ground movement, traffic loading, low temperatures and quality of installation (Lambert and Thornton 2012; Ghorbanian et al. 2015). An Initial estimate of BF_{npd} can be considered as the lower boundary of the data points in a plot that depicting break rates against average zone night pressure (Lambert et al. 2013). Conversely, the BF_{pd} is a function of MPI_{AZP} to the N_2 exponent. Lambert and Thornton (2012) recommended the value of N_2 exponent is recommended to be close to 3 (Lambert and Thornton 2012). As different pipe materials may respond differently to pressure variations, the value of N_2 exponent is estimated for various materials.

The developed BRFs is evaluated by means of model performance indicators, including the coefficient of determination (R^2) and the root mean square error (RMSE). Their mathematical relationships are defined as follows:

$$R^2 = \frac{\left(\sum_{i=1}^n (y_{p,i} - \bar{y}_p)(y_{o,i} - \bar{y}_o)\right)^2}{\sum_{i=1}^n (y_{p,i} - \bar{y}_p)^2 \sum_{i=1}^n (y_{o,i} - \bar{y}_o)^2} \tag{3}$$

$$RMSE = \sqrt{\frac{\sum_{i=1}^n (y_p - y_o)^2}{n}} \tag{4}$$

where y_p = predicted values; y_o = the observed value; \bar{y}_p = the mean of predicted value and \bar{y}_o = the mean of the observed value, and n is the total number of data points.

It should be noted that two simplifications have been considered to develop a BRF. Firstly, each level of the maximum pressure indicator is associated with an average break rate in determining the BRF. Secondly, the maximum pressure is considered to be the only factor controlling pipe break rates (Filion et al. 2007; Ghorbanian et al. 2015). In essence, regarding the break causes, this study focused on the pressure-related pipe breaks. Moreover, the developed BRF may be valid for an individual zone with a group of homogenous pipes, including water mains or service connections with predominant pipe materials under similar environmental conditions (Lambert and Thornton 2012; Ghorbanian et al. 2015). Thus, no effort is made to derive a general relationship between the maximum pressure and pipe break rates for a WDN as a whole in the proposed methodology.

2.3 Identify the MPI Threshold on the BRF

As shown in Fig. 2, there may be an MPI threshold on the developed BRF where for a small increase in threshold may cause a large increase in pipe break rate. The pressure threshold can be identified by a probabilistic approach based on the Bayes theorem. The approach uses pipe breaks data for different pipe materials and pressure heads at the AZP to estimate cumulative distribution functions (CDFs) of the MPI values under normal operation of pressure regime, and when they are coincident with a reported pipe break. These two estimated CDFs are referred to as the unconditional and the break-conditioned CDFs of the MPI, respectively (Martínez-Codina et al. 2015). Subsequently, the estimated CDFs are compared to calculate a probability ratio (PR), which allows the identification of the pressure indicator threshold on the developed BRF.

The hourly average pressure time series at AZP with a moving time window is analyzed to calculate the set of unconditional MPI values. The unconditional CDF of the MPI is then

computed from the calculated set. Furthermore, the set of MPI values conditioned to breaks is obtained using recorded pressure heads before each reported pipe break over a specific time window. Thus, the number of pipe breaks is equal to the number of MPI conditioned to breaks. Eventually, the empirical break-conditioned CDF is estimated by the MPI values conditioned to breaks (Martínez-Codina et al. 2015). It should be noted that the time window to derive the maximum pressure indicator conditioned to breaks include awareness time, which has been reported in the literature between 1 and 3 days (Fanner and Thornton 2005; AWWA 2009; European Commission 2015). Moreover, the selected time window is the same window width used to calculate the set of break-conditioned and unconditional MPI values.

The number of recorded pipe breaks for different pipe materials is often not enough during the time period of data records to estimate the break-conditioned CDF precisely. This may lead to instabilities in the estimation of the probability of pipe breaks (Martínez-Codina et al. 2015). Therefore, this study proposes that the empirical break-conditioned CDF is fitted to a non-parametric break-conditioned CDF, which is estimated by means of the kernel distribution function. The Chi-squared test is then applied to assess whether the non-parametric break-conditioned CDF is followed by the sample of break-conditioned values of the MPI. In this application, the Chi-squared test assesses whether a sample comes from a specified probability distribution function (null hypothesis). The null hypothesis, H_0 , and the alternative hypothesis, H_A , may be written as follows:

$$H_0 = X \rightarrow F_0(x) = F_1(x) \tag{5}$$

$$H_A = X \rightarrow F_0(x) \neq F_1(x) \tag{6}$$

where x = sample values of the MPI conditioned to breaks; $F_0(x)$ = the empirical break-conditioned CDF and $F_1(x)$ = the non-parametric break conditioned CDF. The null hypothesis (H_0) should be rejected at any significance greater than the p value.

The relationship between the estimated CDFs is established by Bayes theorem, which the probability of having a break in a specific time window when the MPI takes a value in the interval $[I_\alpha, I_\beta]$ can be calculated as follows:

$$P(B|I) = \frac{P(I|B).P(B)}{P(I)} \tag{7}$$

where $P(B)$ = the system-wide probability of pipe breaks, $P(I)$ = the probability of the MPI when it is in the interval $[I_\alpha, I_\beta]$, $P(I|B)$ = The conditional probability of the MPI when takes a value in the interval $[I_\alpha, I_\beta]$, if there is a break in a specific time window. Statistically, if the maximum pressure is not influential on pipe break rates, then the conditional probability, $P(I|B)$, and unconditional probability, $P(I)$, are similar and may be independent events, $P(I|B) = P(I)$. Conversely, if these two events are dependent, it may be concluded that maximum pressure may cause a decrease or increase of pipe break rates and $P(I|B) \neq P(I)$. The ratio between them is referred to the probability ratio (PR), which allows the identification of a pressure indicator threshold on the BRF curve and calculated as follows:

$$PR = \frac{P(I|B)}{P(I)} \tag{8}$$

The conditional probability ($P(I|B)$) and unconditional probability ($P(I)$) can be calculated using break-conditioned and unconditional CDFs as follows:

$$P(I) = P(I_\alpha \leq I_i \leq I_\beta) = F_I(I_\beta) - F_I(I_\alpha) \quad (9)$$

$$P(I|B) = P([I_\alpha \leq I_i \leq I_\beta] | B) = F_{I_B}(I_\beta) - F_{I_B}(I_\alpha) \quad (10)$$

where F_I = the unconditional CDFs of the MPI and F_{I_B} = the break-conditioned CDFs of the MPI.

3 Case Study

The proposed methodology is applied to a large zone of the WDN of Tehran, Iran. Figure 3 shows a GIS map of the zone. The network in the zone supplied by gravity and consist of 516 Km length of mains with a total of 9967 individual pipes. The general characteristics of the zone are summarized in Table 1. The mixed main materials of the zone comprise of ductile iron (DI), steel, asbestos cement (AC), polyethylene (PE) and polyvinyl chloride (PVC). As shown in Table 1, the predominant pipe materials are 76% DI and 17% PE, as more than 93% of the mains are made from these materials. Therefore, this work is conducted based on the collected data from DI and PE pipe materials.

Pipe breaks data of the studied zone for a period of 9 years (Mar-2008 to Mar-2017) were collected and filtered from the database. Table 2 shows the number of pipe breaks and annual failure rates (number of breaks/100 km/year) for the selected time periods and pipe materials.

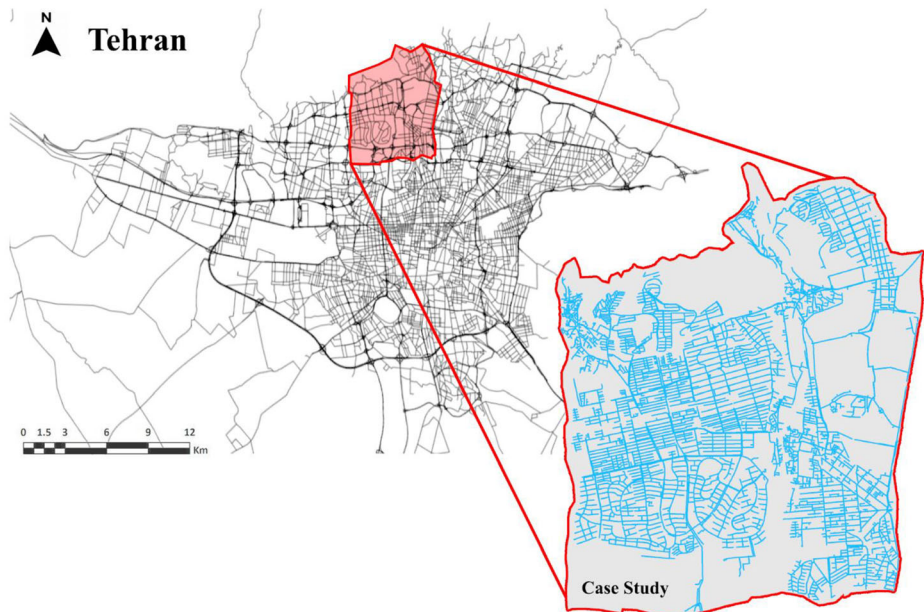


Fig. 3 Representation of the zone considered in this study

Table 1 General characteristics of the study area

| Material | Length by material (Km) | % | Age (year) | Length by age (Km) | % |
|--------------|-------------------------|-------|------------|--------------------|-------|
| DI | 391.9 | 75.96 | 0–10 | 4.34 | 0.84 |
| PE | 88.22 | 17.1 | 10–20 | 56.75 | 11 |
| Steel | 7.69 | 1.5 | 20–30 | 128.96 | 24.99 |
| PVC | 6.21 | 1.2 | 30–40 | 213.45 | 41.37 |
| AC | 5.6 | 1.08 | 40–51 | 95.5 | 18.51 |
| Not. Defined | 16.32 | 3.16 | 51> | 16.95 | 3.29 |
| All | 515.95 | 100 | | 515.95 | 100 |

The periods of time are considered two consecutive years both before and after implementing PM, as it may assist in predicting more precisely the BRFs. It should be mentioned that there was not detailed information about modes of failure for different water mains in the database. Therefore, no attempts were made to associate a failure mode to a recorded pipe break in order to identify and remove those pipe breaks that were not caused by pressure. Moreover, only unintentional pipe breaks were considered in the present study. It should be noted that intentional pipe breaks occur mainly due to the improper execution of construction work, either directly through excavators or indirectly through vibrating construction machines or heavy vehicles.

The GIS tools was exploited to identify the ground level of every service connection within the zone. Subsequently, the WAGL of all service connections was calculated and an appropriate point with ground level close to the calculated WAGL and near the center of the zone was selected as the AZP. Instantaneous pressure values were measured at the AZP of the zone every 15 min. The hourly average pressure heads were then calculated from the average of the four recorded pressure values over each hour. Because of the cyclical behavior of water pressure, the time window was selected 24 h or 1 day (Martínez-Codina et al. 2016). The set of MPI values were obtained from the maximum of hourly average pressure values for each individual day. Subsequently, the maximum and average of the set of the MPI values over 1 year were calculated to develop the BRFs for different pipe materials in the zone. It should be noted that the elevation difference between WAGL and the AZP was added to the obtained values to adjust the MPI values. The WAGL and the AZP elevation were found to be 1545.2 and 1553.1 m, respectively. Table 3 shows the annual maximum and average of the set of MPI values as well as the time period of data records, which is 2 years before and after implementation of PM.

Table 2 pipe break rates before and after pressure management for PE and DI water mains

| Pipe Material | Before PM | | | | After PM | | | |
|---------------|--------------------|-------------------------------|--------------------|-------------------------------|--------------------|-------------------------------|--------------------|-------------------------------|
| | Mar 2008-Mar 2009 | | Mar 2009-Mar 2010 | | Mar 2014-Mar 2015 | | Mar 2015-Mar 2016 | |
| | NO. of pipe breaks | Break rate (No./ 100 Km/year) | NO. of pipe breaks | Break rate (No./ 100 Km/year) | NO. of pipe breaks | Break rate (No./ 100 Km/year) | NO. of pipe breaks | Break rate (No./ 100 Km/year) |
| PE | 113 | 128.08 | 99 | 112.21 | 33 | 37.4 | 45 | 51.01 |
| DI | 39 | 9.95 | 37 | 9.44 | 14 | 3.57 | 12 | 3.06 |

4 Results and Discussion

Following the proposed methodology, the filtered data were used to establish the BRFs for different pipe materials that best fit the data. The BF_{npd} values were estimated using a quick method proposed by Lambert et al. (2013). The estimated values of the BF_{npd} were found to be 23.8 and 1.28 breaks/ 100 km/year for PE and DI, respectively (Table 4). Table 5 shows the developed BRFs and the calculated model performance indicators for PE and DI pipe materials. The graphical plots of the developed BRFs are illustrated in Figs. 4 and 5.

The results provided in Table 5 demonstrate that an improvement for the two performance indicators (R^2 and RMSE) is achieved when the annual average of the MPIs was used to develop the BRFs. More specifically, the comparison of the annual average with the annual maximum of the MPI shows that the improvement for PE and DI pipe materials is 9%, 17% for R^2 and 38.5%, 82% for RMSE, respectively. The improvement achieved can be linked to the fact that the annual average of the MPIs can better represent the failure behavior of water mains. This is because the studied zone is operated under normal pressure regime and often not subject to surges or pressure transients due to supplying the network by gravity with continuous water supply in the time period of the analysis. Moreover, after implementing PM, the reduction of surges and large variations in pressure may cause the MPIs do not interact to the same extent with the other contributing factors to increase the frequency of pipe breaks. Thus, the calculated annual average of the MPIs may be close to those MPI values contributing pipe breaks.

Consequently, the calculated annual average of the MPIs may be an adequate indicator to represent the influence of maximum pressure on the occurrence of pipe breaks. It should be noted that this indicator is not in agreement with the indicator suggested by Lambert and Thornton (2011), which is the maximum static pressure at the AZP, plus any pressure transients and surges over time period (i.e., the annual maximum of the MPIs).

In Table 5, the estimated N_2 values are also given for PE and DI pipe materials. As can be seen, the estimated values of N_2 exponent are significantly different for the two MPIs. The N_2 values for the annual average of the MPIs were found to be higher than by average 60% of the annual maximum of the MPIs. Additionally, the estimated values of N_2 exponent for the annual average of the MPIs are near the suggested value for the N_2 exponent (i.e., close to 3) in other studies (Lambert and Thornton 2012; Lambert et al. 2013). Furthermore, the N_2 values for the selected pipe materials should be noticed. As shown in Table 5, the estimated values of N_2 exponent for PE are higher than the DI material. One conclusion derived from the results is that maximum pressure is more influential on pressure-dependent pipe break rates for PE pipe materials. As a consequence, N_2 value would be dependent on pipe material, and may be

Table 3 The calculated MPI values for the studied zone before and after PM

| | Data records | Annual maximum of MPI (m) | Annual average of MPI (m) | Elevation difference (m) | Adjusted annual maximum of MPI at AZP (m) | Adjusted annual average of MPI at AZP (m) |
|-----------|-------------------|---------------------------|---------------------------|--------------------------|---|---|
| Before PM | Mar 2008-Mar 2009 | 90.4 | 61.6 | 7.9 | 98.3 | 69.5 |
| | Mar 2009-Mar 2010 | 70.9 | 61.3 | | 77.9 | 69.2 |
| After PM | Mar 2014-Mar 2015 | 38.7 | 33.2 | | 46.6 | 41.1 |
| | Mar 2015-Mar 2016 | 36.6 | 33.6 | | 44.5 | 41.5 |

Table 4 Estimation of BF_{npd} for PE and DI water mains

| Pipe Material | Before PM | | | | After PM | | | |
|---------------|-------------------|--------------------------------------|-------------------|--------------------------------------|-------------------|--------------------------------------|-------------------|--------------------------------------|
| | Mar 2008-Mar 2009 | | Mar 2009-Mar 2010 | | Mar 2014-Mar 2015 | | Mar 2015-Mar 2016 | |
| | AZNP (m) | BF _{npd} (No./ 100 Km/year) | AZNP (m) | BF _{npd} (No./ 100 Km/year) | AZNP (m) | BF _{npd} (No./ 100 Km/year) | AZNP (m) | BF _{npd} (No./ 100 Km/year) |
| PE | 75.8 | 37.4 | 74.5 | 23.8 | 44.2 | 27.2 | 43.8 | 31.3 |
| DI | | 3.06 | | 1.28 | | 2.12 | | 2.55 |

different for each material. Therefore, if there is no scarcity of pipe breaks data, the value of N_2 exponent should be estimated for each pipe material separately in an individual zone.

Over period of years, the slope of the developed BRF curves in the pressure-dependent part may increase because of influential factors contributing to pipe breaks such as age, corrosion, operating characteristics, climate and soil conditions (Thornton and Lambert 2007). Moreover, some local conditions of the zone, including ground movement, traffic loading, quality of installation, and seasonal influences, may change the non-pressure dependent pipe break rates (Creaco and Walski 2017). Therefore, a unique BRF should be provided under similar operational and environmental conditions in a zone for each type and pipe material when sufficient field data is available to obtain a robust statistical analysis. In addition, the determination of the BRFs should be periodically updated to incorporate the changing conditions of the network.

The predicted reduction of pipe break rates (R) for PE, and DI pipe materials are presented in Table 6. It should be mentioned that the C_b values were calculated using the estimated B_{Fnpd} , and the actual pipe breaks before PM (BF_0). The obtained C_b values were found to be 0.2 and 0.13 for PE and DI materials, which can be explained in terms of pipe ages. The C_b usually has higher values in new networks because the more numbers of pipe breaks in new WDNs would not be directly related to pressure and may be associated with BF_{npd} . Conversely, in old WDNs, the more numbers of pipe breaks are usually associated with pressure-related failures, and thus, C_b has lower values (Lambert et al. 2013; Creaco and Walski 2017). The estimated reduction of pipe breaks (R) was found to be 63.31%, 61.8% for PE, DI pipe materials, respectively (Table 6). The estimated values for pipe breaks reductions can be explained in terms of C_b values and the reduction of the maximum operating pressures, which can cause significant reductions of pipe breaks in the zone Table 6 shows that the predicted reductions of pipe breaks will reach values around 60% if the MPI is decreased around 40%. These results

Table 5 the developed BRFs for the selected pipe materials in the study area

| Pipe material | MPI | BRF | A parameter | N_2 | Coefficient of determination (R^2) | RMSE |
|---------------|--------------------|--|-------------|-------|--|-------|
| PE | Annual Max of MPI | $BF = 23.8 + A \times MPI_{AZP}^{N_2}$ | 0.0229 | 1.85 | 0.871 | 16.04 |
| | Annual Avg. of MPI | | 0.000286 | 3.11 | 0.951 | 9.86 |
| DI | Annual Max of MPI | $BF = 1.28 + A \times MPI_{AZP}^{N_2}$ | 0.00489 | 1.51 | 0.852 | 1.34 |
| | Annual Avg. of MPI | | 0.00031 | 2.41 | 0.995 | 0.24 |

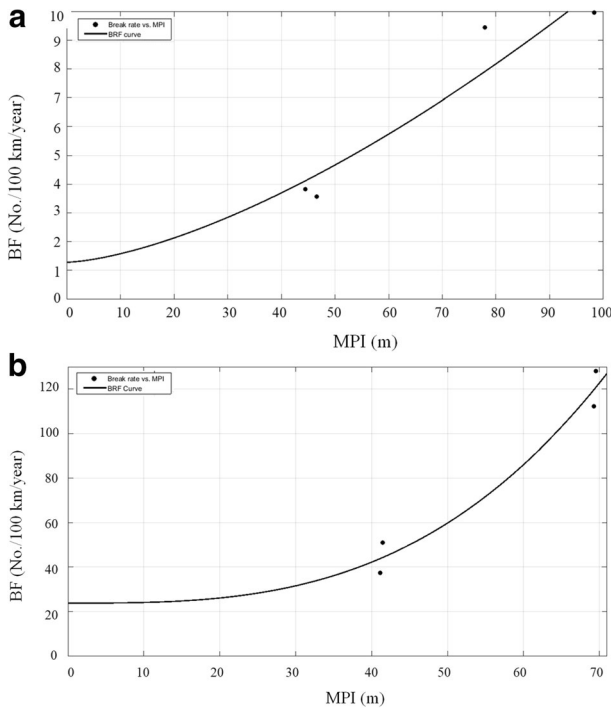


Fig. 4 Break rate function for PE material using **a)** Annual maximum of the MPI values; **b)** Annual average of the MPI values

suggest that the reduction of maximum pressure is significantly influential on the reductions of pipe break rates in the study area.

In the last part of the methodology, after the BRFs were developed, the maximum pressure thresholds on the BRFs are identified where pipe break rate increases rapidly for small pressure increases. For this reason, the Bayes theorem was applied to determine a pressure ratio that compares the probability distribution of unconditional and break-conditioned of the MPI.

The set of the unconditional MPI values as a random variable was used to derive the unconditional CDF. Moreover, the empirical break-conditioned CDF was estimated by the MPI values conditioned to breaks. It should be noted that the time window used to determine the MPI values were selected 1 day. As the number of pipe breaks for the selected pipe materials is not long enough to estimate the break-conditioned CDF precisely, the empirical break-conditioned CDF was fitted to a non-parametric kernel distribution to determine the probability distribution of the MPI conditioned to breaks. In order to assess whether the break-conditioned distribution follows the same non-parametric kernel distribution function in the fitting, the Chi-squared test was applied. Table 7 presents the test results at 95% confidence level and the non-parametric CDF parameters for the zone.

As shown in Table 7, the results of the Chi-squared test demonstrate that *p* values is above 0.05 for PE and DI materials. This is inferred from the result that the probability distribution functions of the MPIs conditioned to breaks are reproduced quite well by the non-parametric distribution function, at a confidence level of 95%. Figure 6 graphically represents the unconditional CDF, the empirical break-conditioned CDF, and the non-parametric break-

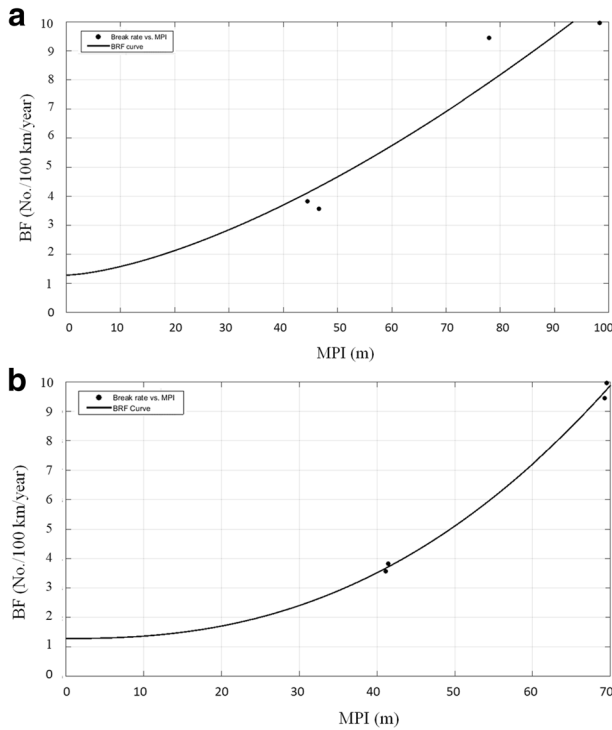


Fig. 5 Break rate function for DI material using **a)** Annual maximum of the MPI values; **b)** Annual average of the MPI values

conditioned CDF of the MPI values for the PE and DI pipe materials. In order to compute the unconditional and break-conditioned probabilities of the MPI, the total range of the MPI on the developed BRFs was divided into 17 pressure intervals with equal length. The probability of the MPI for a specific pressure interval $[I_{\alpha}, I_{\beta}]$ was then calculated using the unconditional and the non-parametric break-conditioned CDFs. Subsequently, the probability ratio (PR) was determined using the ratio between the computed probability of the unconditional and break-conditioned MPI in each pressure interval. Figure 7 shows the calculated PR values for PE and DI materials in the zone. The unit PR is distinguished by the horizontal solid line. This is inferred from the result that the maximum pressure clearly influences the probability of the occurrence of pipe breaks and increases the pipe failure rates, as the probability ratio is greater than 1 for certain maximum pressure ranges. At a practical level, these ranges should be avoided to reduce pipe break rates and implement effective PM in the zone. Conversely, the reduction of maximum pressure has will not necessarily result in decreasing pipe breaks when the probability ratio is smaller than 1. However, the residual working life of pipes can be extended, as it is explained in other studies (Thornton and Lambert 2007; Lambert and

Table 6 The reduction of pipe breaks for PE and DI materials

| Pipe material | BF _{n_{pd}} | BF ₀ | C _b | N ₂ exponent | Pressure reduction (%) | Pipe breaks reduction (%) |
|---------------|------------------------------|-----------------|----------------|-------------------------|------------------------|---------------------------|
| PE | 23.8 | 120.1 | 0.2 | 3.11 | 40.5 | 63.3 |
| DI | 1.28 | 9.95 | 0.13 | 2.41 | 40.5 | 61.8 |

Table 7 Test results (*p* value) of the Chi-squared test for the empirical break-conditioned CDF of the MPI at the 95% confidence level for the zone

| | Non-parametric CDF | CDF parameters | | p value | Chi-squared test (accepted) |
|----|--------------------|-----------------------------------|---------------|---------|-----------------------------|
| PE | Kemel Distribution | Kernel Smooth Func. Band Width | Normal 0.6 | 0.1711 | Yes |
| DI | Kemel Distribution | Kernel Smooth Func. Band Width | Normal 0.5 | 0.2218 | Yes |

Thornton 2011; Lambert et al. 2013). As can be seen in Fig. 7, all PRs do not follow a definite or regular trend, although it is expected an increment trend with increasing maximum pressure values. This may be due to the fact that pipe breaks data is not long enough that the probability distribution of pipe breaks can be estimated precisely.

A pressure indicator threshold could be identified in Fig. 7, which corresponds to the first maximum pressure range that crosses the unit PR. These thresholds were found 31 and 36 m pressure head for PE and DI materials, respectively, in the study area. As can be expected, the larger value of thresholds is related to DI materials. This can be related to the fact that DI pipe material may provide more resistance against maximum pressure causing pipe breaks. Moreover, the differences between the calculated pressure thresholds can be explained in terms of the concept of failure envelopes, which is a function of pipe materials (Pearson et al. 2005). As mentioned previously, over the period of years, the BRFs may vary because of changing in

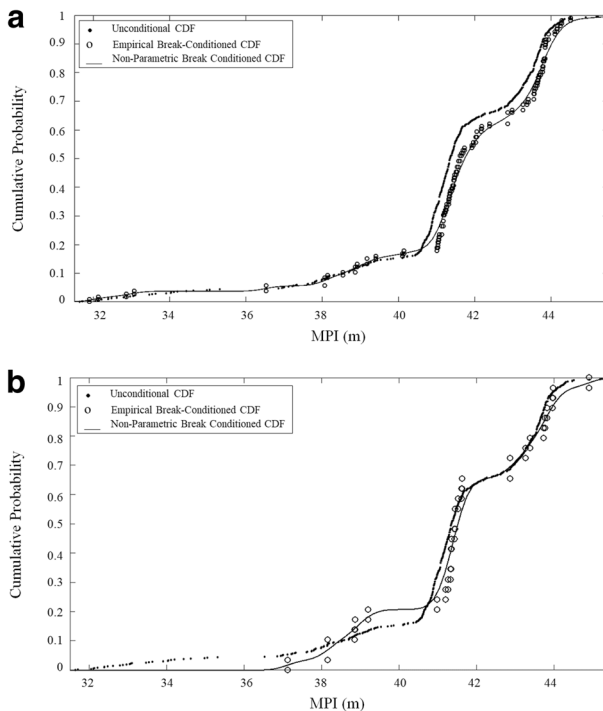


Fig. 6 **a** The estimated CDFs of the MPI values for PE pipe material; **b** The estimated CDFs of the MPI values for DI pipe material. Unconditional CDF (dots), empirical break-conditioned CDF (open circle) and non-parametric break conditioned CDF (solid line)

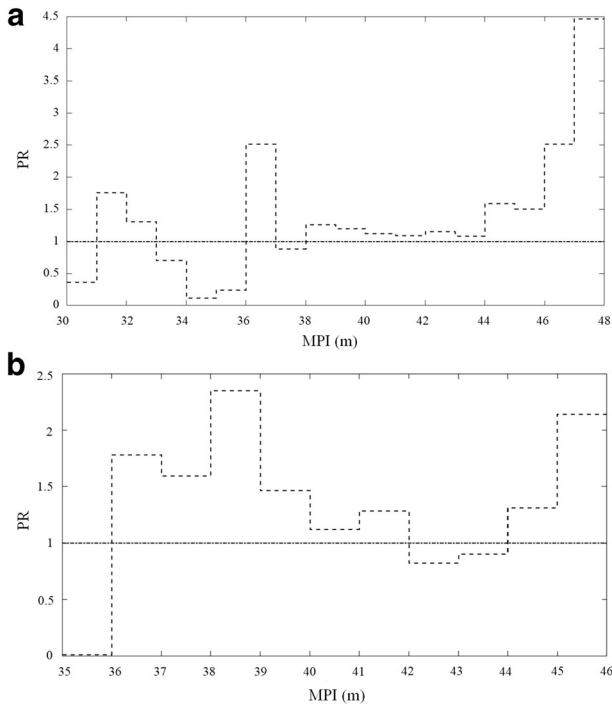


Fig. 7 The calculated PR values on the maximum pressure range **a** for PE material; **b** for DI material

zone conditions, operating pressure, and combination of influential factors contributing to pipe breaks like pipe deterioration, low temperatures, and traffic loading. Furthermore, the break-conditioned CDFs of MPIs need to be periodically estimated, as each pipe material may respond differently to changes in maximum pressures. For all these reasons, the maximum pressure thresholds should be identified for the BRFs with homogenous pipes (type and material) under similar environmental and operational conditions.

There are some limitations to apply the proposed methodology. First, no attempt was made to derive a general BRF for a whole WDN. On the other hand, the objective of this study is to determine the BRFs for an individual zone of a WDN and for different materials in order to assess the response of each zone to the reduction of maximum pressure. Second, this study is unable to consider pipe breaks due to short term hydraulic transients, as pressure data were collected at 15-min intervals. Third, there was no segregated pipe breaks data based on failure modes, as such data were not available in the database. Therefore, BF_{npd} was estimated based on all data of pipe breaks, and no attempt was made to remove the pressure-related pipe breaks. Additionally, for the same reason, all pipe breaks data was used to determine the BRFs. This may increase the statistical noise in data, which can be a source of error in determining BRFs and can prevent a robust statistical inference. Forth, the maximum pressure is considered to be a key control parameter in occurrences of pipe breaks. Thus, this parameter coupled with other physical and environmental factors, can increase pipe break rates. Fifth, The BRFs and the pressure thresholds on them may be valid for homogenous pipes (type and material) under similar operational and environmental conditions. Therefore, when these conditions change, the analysis should be repeated.

5 Conclusions

A practical field data-based methodology was presented to determine the BRFs with the objective of exploring the relationship between pressure and pipe breaks in WDNs. The methodology was applied to a large zone of the WDN of Teheran (Iran). The AZP was determined based on a four-step systematic approach, and the MPI values were calculated using the measured pressure heads at the AZP over a specific time window. The BRFs were determined through the analysis of the MPI values, and the filtered pipe breaks data for each pipe material. The results showed that the annual average of the MPI could better represent the failure behavior of water mains. Both the performance indicators (R^2 and RMSE) were improved when this indicator was used to determine the BRFs. The estimated N_2 exponent for PE and DI materials were found 3.11 and 2.41, confirming that N_2 exponent would be dependent to pipe materials. Thus, if sufficient field data is available, the BRFs and also N_2 exponent should be estimated separately for each pipe of material. The results also demonstrated that, on average, the % reduction in pipe breaks was 1.5 times the % reduction in maximum pressure in the study area. The determined BRFs can be used to evaluate the associated benefits of PM for the development of economic models.

The pressure threshold on the obtained BRFs were identified based on a Bayes theorem which corresponds to the first maximum pressure ranges that crosses the unit PR. The probability distribution functions of unconditional and break-conditioned of the MPI values were computed to identify the PR values. The first one was used to derive the unconditional CDF of the MPI. The empirical break-conditioned CDF was also estimated by the second probability distribution. It was then fitted to a non-parametric CDF estimated by means of the kernel distribution function, as the number of pipe breaks in not long enough to estimate the probability of the MPI conditioned to breaks precisely. The results of Chi-squared test indicated that the probability distribution of the MPI conditioned to breaks were reproduced quite well by the non-parametric CDF, at a confidence level of 95% for PE and DI pipe materials.

The results of this paper pointed out that the pipe break rates may increase for specific maximum pressure ranges above the maximum pressure thresholds where the PR values are greater than 1. Conversely, when the PR smaller than 1, the reduction of maximum pressure does not necessarily affect on decreasing of pipe break rates, however, the residual life of pipes would be extended. The maximum pressure thresholds on the BRFs were found 31 and 36 m for PE and DI materials. The differences between these thresholds can be explained in terms of the concept of the failure envelope, which is the function of pipe materials. At a practical level, the MPI values should be limited to the obtained thresholds to implement effective PM and reduce pipe break rates as far as possible in the zone. The results of this paper suggest that the BRFs and pressure thresholds on them should be determined for homogenous pipes (type and material) under similar physical and operational conditions. Moreover, they should be updated periodically as the conditions of the zone, and operating pressure can change over the period of years. In the methodology presented here, the usage of commercial packages like HYTRAN for evaluating hydraulic transients causing pipe breaks may be explored. Furthermore, other pressure indicators related to pipe breaks like pressure range, pressure variability, and pressure variation rate may be investigated and tested to improve the results.

Compliance with Ethical Standards

Conflict of Interest No conflict of interest.

References

- Al-Barqawi H, Zayed T (2006) Condition rating model for underground infrastructure sustainable water mains. *J Perform Constr Facil* 20:126–135. [https://doi.org/10.1061/\(ASCE\)0887-3828\(2006\)20:2\(126\)](https://doi.org/10.1061/(ASCE)0887-3828(2006)20:2(126))
- AWWA (2009) Water audits and loss control programs - manual of water supply practices, 3rd ed. Denver
- Babovic V, Keijzer M, Hansen PF (2002) A data mining approach to modelling of water supply assets. *Urban Water J* 4:401–414
- Berardi L, Giustolisi O, Kapelan Z, Savic DA (2008) Development of pipe deterioration models for water distribution systems using EPR. *J Hydroinf* 10:113–126. <https://doi.org/10.2166/hydro.2008.012>
- Creaco E, Walski T (2017) Economic analysis of pressure control for leakage and pipe burst reduction. *J Water Resour Plan Manag* 143:04017074. [https://doi.org/10.1061/\(ASCE\)WR.1943-5452.0000846](https://doi.org/10.1061/(ASCE)WR.1943-5452.0000846)
- European Commission (European Union) (2015) EU reference document good practices on leakage management WFD CIS WG PoM, Main report. Luxembourg: Office for Official Publications of the European Communities
- Fanner P, Thornton J (2005) The importance of real loss component analysis for determining the correct intervention strategy. *Proc IWA spec Conf “leakage 2005”* 1–11
- Farley M, Trow S (2003) Losses in water distribution networks: a practitioner’s guide to assessment, monitoring and control
- Filion YR, Adams BJ, Karney B (2007) Stochastic Design of Water Distribution Systems with expected annual damages. *J Water Resour Plan Manag* 133:244–252
- Ghorbanian V, Guo Y, Karney B (2015) Field data – based methodology for estimating the expected pipe break rates of water distribution systems. *J Water Resour Plan Manag* 142:1–11. [https://doi.org/10.1061/\(ASCE\)WR.1943-5452.0000686](https://doi.org/10.1061/(ASCE)WR.1943-5452.0000686)
- Girard M, Stewart RA (2007) Implementation of pressure and leakage management strategies on the Gold Coast, Australia: case study. *J Water Resour Plan Manag* 133:210–217. [https://doi.org/10.1061/\(ASCE\)0733-9496\(2007\)133:3\(210\)](https://doi.org/10.1061/(ASCE)0733-9496(2007)133:3(210))
- Giustolisi O, Savic DA (2006) A symbolic data-driven technique based on evolutionary polynomial regression. *J Hydroinf* 8:207–222. <https://doi.org/10.2166/hydro.2006.020>
- Giustolisi O, Savic DA (2009) Advances in data-driven analyses and modelling using EPR-MOGA. *J Hydroinf* 11:225–236. <https://doi.org/10.2166/hydro.2009.017>
- ILMSS (International Leakage Management Support Services) (2013) Guidelines relating to the assessment and calculation of average pressure in water distribution systems and zones. Gwynedd, UK: ILMSS.
- Jafar R, Shahroui I, Juran I (2010) Application of artificial neural networks (ANN) to model the failure of urban water mains. *Math Comput Model* 51:1170–1180. <https://doi.org/10.1016/j.mcm.2009.12.033>
- Kabir G, Demissie G, Sadiq R, Tesfamariam S (2015) Integrating failure prediction models for water mains : Bayesian belief network based data fusion. *Knowledge-Based Syst* 85:159–169. <https://doi.org/10.1016/j.knsys.2015.05.002>
- Kabir G, Tesfamariam S, Asce M, et al (2010) Integrating Bayesian linear regression with ordered weighted averaging : uncertainty analysis for predicting water Main failures. doi: <https://doi.org/10.1061/AJRU6.0000820>
- Kabir G, Tesfamariam S, Francisque A, Sadiq R (2015) Evaluating risk of water mains failure using a Bayesian belief network model. *Eur J Oper Res* 240:220–234. <https://doi.org/10.1016/j.ejor.2014.06.033>
- Kabir G, Tesfamariam S, Loeppky J, Sadiq R (2016) Predicting water main failures: a Bayesian model updating approach. *Knowledge-Based Syst* 110:144–156. <https://doi.org/10.1016/j.knsys.2016.07.024>
- Kakoudakis K, Behzadian K, Farmani R, Butler D (2017) Pipeline failure prediction in water distribution networks using evolutionary polynomial regression combined with K-means clustering. *Urban Water J* 14:737–742. <https://doi.org/10.1080/1573062X.2016.1253755>
- Kleiner Y, Rajani B (2001) Comprehensive review of structural deterioration of water mains: statistical models. *Urban Water* 3:131–150. [https://doi.org/10.1016/S1462-0758\(01\)00033-4](https://doi.org/10.1016/S1462-0758(01)00033-4)
- Kutyłowska M (2015) Neural network approach for failure rate prediction. *Eng Fail Anal* 47:41–48. <https://doi.org/10.1016/J.ENGFAILANAL.2014.10.007>
- Lambert A (2001) What do we know about pressure: leakage relationships in distribution systems? In: IWA Conference. pp 1–8
- Lambert AO (2002) International report: water losses management and techniques. *Water Sci Technol Water Supply* 2:1–20
- Lambert AO, Fantozzi M (2010) Recent developments in pressure management. *Proc IWA Int spec Conf “water loss 2010”*
- Lambert A, Fantozzi M, Thornton J (2013) Practical approaches to modelling leakage and pressure management in distribution systems - progress since 2005. In: 12th international conference on computing and control for the water industry

- Lambert A, Thornton J (2011) The relationships between pressure and bursts – a ‘state-of-the-art’ update. *water* 21 J
- Lambert A, Thornton J (2012) Pressure: bursts relationships: influence of pipe materials, validation of scheme results, and implications of extended asset life. In: *Water Loss* 2012. pp 2–11
- Martínez-Codina Á, Cueto-Felgueroso L, Castillo M, Garrote L (2015) Use of pressure management to reduce the probability of pipe breaks: a Bayesian approach. *J Water Resour Plan Manag* 141:04015010. [https://doi.org/10.1061/\(ASCE\)WR.1943-5452.0000519](https://doi.org/10.1061/(ASCE)WR.1943-5452.0000519)
- Martínez-Codina CM, González-Zeas D, Garrote L (2016) Pressure as a predictor of occurrence of pipe breaks in water distribution networks. *Urban Water J* 13:676–686. <https://doi.org/10.1080/1573062X.2015.1024687>
- Moslehi I, Jalili_Ghazizadeh M, Yousefi_Khoshqalb E, (2020) Developing a framework for leakage target setting in water distribution networks from an economic perspective. *Structure and Infrastructure Engineering*. <https://doi.org/10.1080/15732479.2020.1777568>
- Nishiyama M, Filion Y (2013) Review of statistical water main break prediction models. *Can J Civ Eng* 40:972–979. <https://doi.org/10.1139/cjce-2012-0424>
- Palau CV, Arregui FJ, Carlos M (2012) Burst detection in water networks using principal component analysis. *J Water Resour Plan Manag* 138:47–54. [https://doi.org/10.1061/\(ASCE\)WR.1943-5452.0000147](https://doi.org/10.1061/(ASCE)WR.1943-5452.0000147)
- Pearson D, Fantozzi M, Soares D, Waldron T (2005) Searching for N2: how does pressure reduction reduce burst frequency? *Proc IWA Spec Conf Leakage* 2005:1–14
- Rajani B, Kleiner Y (2001) Comprehensive review of structural deterioration of water mains: physically based models. *Urban Water* 3:151–164. [https://doi.org/10.1016/S1462-0758\(01\)00032-2](https://doi.org/10.1016/S1462-0758(01)00032-2)
- Renaud E, Sissoko MT, Clauzier M et al (2015) Comparative study of different methods to assess average pressures in water distribution zones. *Water Util J* 10:25–35
- Scheidegger A, Leitão JP, Scholten L (2015) Statistical failure models for water distribution pipes – a review from a unified perspective. *Water Res* 83:237–247. <https://doi.org/10.1016/j.watres.2015.06.027>
- Shirzad A, Tabesh M, Farmani R (2014) A comparison between performance of support vector regression and artificial neural network in prediction of pipe burst rate in water distribution networks. *KSCE J Civ Eng* 18: 941–948. <https://doi.org/10.1007/s12205-014-0537-8>
- Thornton J, Lambert A (2005) Progress in practical prediction of pressure : leakage , pressure : burst frequency and pressure : consumption relationships. In: *Proceedings of IWA Special Conference “Leakage 2005.”* Halifax, Canada, pp 1–10
- Thornton J, Lambert A (2006) Managing pressures to reduce new breaks. *J Water* 21:24–26
- Thornton J, Lambert A (2007) Pressure management extends infrastructure life and reduces unnecessary energy costs. In: *water loss 2007*. Bucharest -Romania
- Vicente DJ, Garrote L, Sánchez R, Santillán D (2016) Pressure Management in Water Distribution Systems: current status, proposals, and future trends. *J Water Resour Plan Manag* 142:04015061. [https://doi.org/10.1061/\(ASCE\)WR.1943-5452.0000589](https://doi.org/10.1061/(ASCE)WR.1943-5452.0000589)
- Wang Y, Zayed T, Moselhi O (2009) Prediction models for annual break rates of water mains. *J Perform Constr Facil* 23:47–54. [https://doi.org/10.1061/\(ASCE\)0887-3828\(2009\)23:1\(47\)](https://doi.org/10.1061/(ASCE)0887-3828(2009)23:1(47))
- WSAA (Water Services Association of Australia) (2009) Guidelines relating to the calculation of Average Pressures in Water Distribution Systems and Zones. Prepared by Wide Bay Water Corporation for Water Services Association of Australia, as part of WSAA Asset Monitoring Project PPs-3, jaimie.hicks@wsaa.as
- Xu Q, Chen Q, Li W (2011) Application of genetic programming to modeling pipe failures in water distribution systems. *J Hydroinfr* 13:419–428. <https://doi.org/10.2166/hydro.2010.189>
- Xu Q, Chen Q, Li W, Ma J (2011) Pipe break prediction based on evolutionary data-driven methods with brief recorded data. *Reliab Eng Syst Saf* 96:942–948. <https://doi.org/10.1016/j.ress.2011.03.010>

Publisher’s Note Springer Nature remains neutral with regard to jurisdictional claims in published maps and institutional affiliations.